

# Drone Assisted Flying Ad-Hoc Networks: Mobility and Service Oriented Modeling using Neuro-Fuzzy

Kirshna Kumar <sup>a</sup>, Sushil Kumar <sup>a</sup>, Omprakash Kaiwartya<sup>b</sup>, Pankaj Kumar Kashyap<sup>a</sup>, Jaime Lloret<sup>c</sup>, Houbing Song<sup>d</sup>

<sup>a</sup> School of Computer and Systems Sciences, Jawaharlal Nehru University, New Delhi, India.

(e-mail: [kirshn44\\_scs@jnu.ac.in](mailto:kirshn44_scs@jnu.ac.in), [skdohare@mail.jnu.ac.in](mailto:skdohare@mail.jnu.ac.in), [pankaj76\\_scs@jnu.ac](mailto:pankaj76_scs@jnu.ac) ).

<sup>b</sup>School of Science and Technology, Nottingham Trent University, Clifton Campus, NG11 8NS, Nottingham, UK. email: [omprakash.kaiwartya@ntu.ac.uk](mailto:omprakash.kaiwartya@ntu.ac.uk)

<sup>c</sup>Integrated Management Coastal Research Institue, Universitat Politecnica de Valencia, Spain. Email: [jlloret@com.upv.es](mailto:jlloret@com.upv.es)

<sup>d</sup>Houbing Song is with the Embry-Riddle Aeronautical University, USA. Email: SONGH4@erau.edu

## Abstract

Flying ad-hoc networks enable vast of IoT services while maintaining communication among the ground systems and flying drones. The domain research is focusing on flying networks assisted data centric IoT applications while integrating the benefits and services of aerial objects such as unmanned aerial vehicle and drones. Considering the growing market significance of drone centric flying networks, quality of service provisioning is one of the most leading research themes in flying ad-hoc networks. The related literature majorly relies on centralized base station monitored communications. Towards this end, this paper proposes a drone assisted distributed routing framework focusing on quality of service provision in IoT environments (D-IoT). The aerial drone mobility and parameters are modeled probabilistically focusing on highly dynamic flying ad-hoc networks environments. These drone centric models are utilized to develop a complete distributed routing framework. Neuro-fuzzy interference system has been employed to assist in reliable and efficient route selection. A comparative performance evaluation attests the benefits of the proposed drone assisted routing framework. It is evident that D-IoT outperforms the state-of-the-art techniques in terms of number of network performance metrics in flying ad-hoc networks environments.

## Keywords

Flying ad-hoc networks, Internet of Things, Quality of Service, Routing, Aerial drone

## 1. Introduction

Internet of Things (IoT) is one of the leading research domains in recent years due to the growing applicability in different new areas [1, 2]. The novel domains such as smart healthcare, smart home/city, intelligent transportation, Unmanned Aerial Vehicles (UAVs) simulation [3], pollution monitoring, disaster management, industrial IoT, smart agriculture have emerged as prominent themes to revolutionize IoT in day to day life [4-6]. In aeronautical applications, for transmitting and viewing data immediately, Internet is utilized to connect actuators and sensors inside the aerial objects. After the trip completion, data related to flight would be tracked in real-time with the usage of IoT devices and technologies in place for downloading data from sensors [7]. Currently, usage of sensors and actuators through novel technologies such as drone assisted Flying Ad-Hoc networks (FANET) plays a prominent role in smart agriculture [8]. The application of Drone assisted Flying Ad-Hoc networks makes current agriculture smarter by overcoming the various challenges of farmers such as sudden climate changes, disease and pest detection of crops and the presence of parasites [9,10].

Fig.1 illustrates the different aerial communication systems: satellite communication, air-ground and air-air communication. It is highlighted that drone controller is a specific drone with higher computing and communication capability which works as coordinator in aerial adhoc network

Cite As:

Kumar, K., Kumar, S., Kaiwartya, O., Kashyap, P.K., Lloret, J. and Song, H., 2020. Drone assisted flying ad-hoc networks: mobility and service oriented modeling using neuro-fuzzy. *Ad Hoc Networks*, 106, p.102242.

environment. In satellite-based communication system, aerial object such as drone accesses Internet and remains in contact with ground while utilizing satellite as a relay node to cover remote, ocean or polar areas [11]. But these satellite-based centralized aerial communication systems have higher operation and maintenance cost. While comprising multi hop ad hoc networking among the drones, extension of network architecture is known as Flying ad hoc network [12]. While permitting and maintaining communication between drone and ground, over the region without communication infrastructure, flying ad hoc network can be utilized as a complementary communication system. Flying ad hoc network facilitates Internet reachability to these drones while traversing via these areas, with no usage of costly satellite links and high delay [13]. Therefore, in this paper, we focus only on flying ad hoc network and ground communication without involvement of satellite system. However, providing reliable and stable communication among drone and ground stations in flying ad hoc network assisted flight communication system is a great challenge [14].

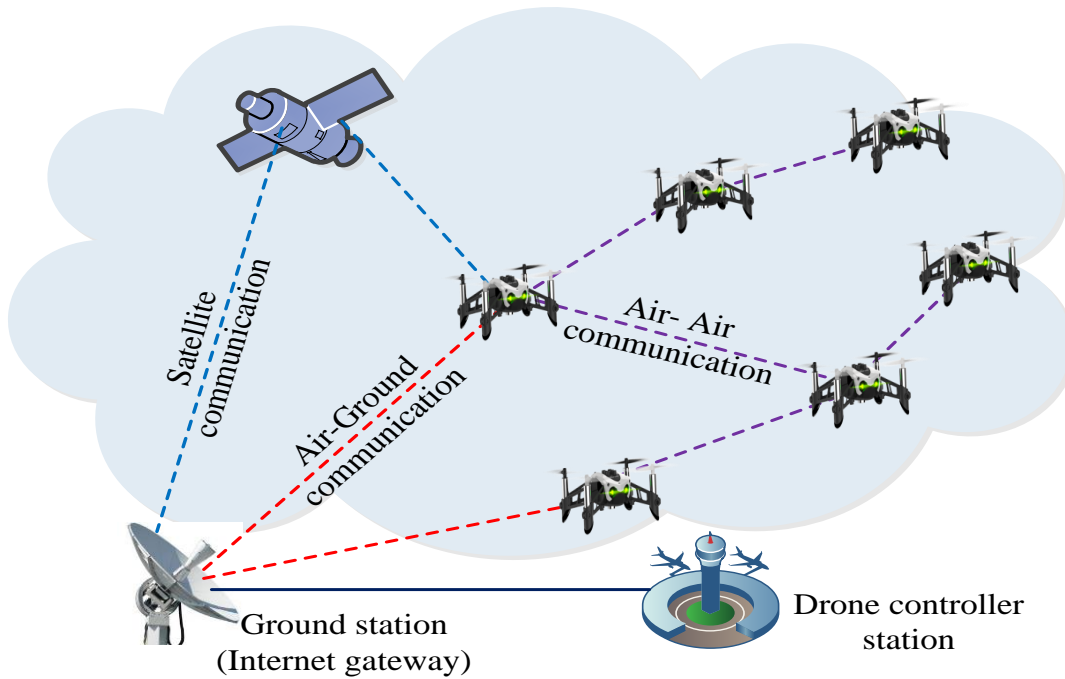


Fig.1. Aerial communication systems

In High speed mobility of drones in flying ad hoc networks is the key challenge in ad-hoc aerial communication. It causes variation in network topology in frequent and unpredictable manner, which results in link breakage in multi hop communication [15]. Consequently, the performance of flying ad hoc network degrades in terms of reliability. The requirement of drone networks having efficient quality of service (QoS) parameters motivates to design a drone assisted distributed routing framework focusing on quality of service provision in drone assisted IoT environments (D-IoT). Towards this end, in this paper we propose a drone assisted distributed routing framework focusing on quality of service provision to maximize network performance inside D-IoT environment. Additionally, we compute route availability factor, residual route load capacity and route delay as the route selection metric for the purpose of QoS provisioning while selecting the optimized route. Neuro-fuzzy inference system has been implemented to find the aggregated output based on QoS metrics route availability factor, residual route load capacity and route delay. The advantage of using hybrid structure; neural network with fuzzy logic counterbalance each other's such as generalization to environment is done by neural network learning procedure (change the inbuilt rule of fuzzy logic) and error is minimized. Whereas simplification of output generated by fuzzy inference system in quick time [43]. Hence, a route having stability and properly balance traffic can be selected between drone and ground stations. Further, a best advertisement forwarding (BADF) technique is utilized to reduce the overhead related to advertisement flooding generated during route selection process.

Cite As:

Kumar, K., Kumar, S., Kaiwartya, O., Kashyap, P.K., Lloret, J. and Song, H., 2020. Drone assisted flying ad-hoc networks: mobility and service oriented modeling using neuro-fuzzy. *Ad Hoc Networks*, 106, p.102242.

Then, D-IoT and state-of-the-art protocols are evaluated and compared. The key contributions of the paper can be summarized as follows:

- 1) A network model for drone assisted IoT environment is presented focusing the topological aspects of aerial drones and its mobility in flying adhoc networks.
- 2) To optimize Drone network centric QoS provisioning parameters are derived focusing on relative velocity of drones, expected link availability period, residual route load capacity and route delay.
- 3) Neuro-fuzzy interference system has been employed to jointly combine three important QoS provisioning parameters to assist in reliable and efficient route selection.
- 4) A drone assisted distributed routing framework is developed based on the drone mobility model and QoS parameters.
- 5) The proposed communication framework is tested to comparatively evaluate the performance with the state-of-the-art protocols considering metrics related to flying ad-hoc networks environments.

The remainder of this paper is structured as follows. Section II introduces related literatures of recent QoS- non provisioning and QoS- aware routing techniques for flying ad hoc networks. In Section III, the details of the proposed drone assisted distributed routing framework (D-IoT) is presented. Section IV discusses the implementation and analysis of simulation results. Conclusion is presented in Section V.

## 2. Related work

In this section, related literature on routing in flying ad-hoc networks has been reviewed while focusing on QoS non provisioning routing and QoS aware routing.

### 2.1 QoS non- provisioning routing

Two novel stability driven clustering schemes have been proposed while establishing stable clusters for highly mobile ad hoc networks comprising ships, aircraft, cars and trains as mobile nodes [18]. For the scenarios with unknown position information of mobile nodes, first scheme is utilized and for the scenarios with known position information (via GPS), second scheme is utilized. This scheme lacks data reliability. An automatic dependent surveillance broadcast system based geographical routing has been suggested while utilizing aircraft position and velocity to remove beaconing of traditional routing [19]. In this scheme, next hop has been selected based on aircraft velocity metric while adaptively coping with highly dynamic aircraft and network topology. This scheme does not focus on providing optimized load capacity. Reactive greedy reactive routing has been proposed for highly mobile and density variable unmanned aerial vehicle communication systems while combining the characteristics of reactive routing techniques with geographical routing techniques [20]. In this scheme, velocity vector-based mobility prediction technique has been utilized to predict the aircraft location and two various scoped flooding techniques have been used while reducing message overhead. This scheme lacks the Quality of service metrics such as delay and link lifetime. An unmanned aerial vehicle-based communication system while providing connectivity and deployment modules for emergency disaster recovery has been proposed [21]. This system comprises three prominent sub system such as navigation system, communication sub system and schemes for formation management. The parameters such as link availability, jitter, throughput and packet loss have not been considered in the communication system. A two-echelon ground vehicle and its mounted drone co-operative routing technique (2E-GUCRP) has been proposed for intelligence, surveillance, and reconnaissance (ISR) missions while minimizing the overall mission time to meet the operational constraints [22]. QoS constraints are not utilized in this routing technique. A glowworm swarm optimization and dragonfly approach-based hybrid self-organized clustering protocol has been proposed for drone assisted cognitive IoT networks [23]. After introducing cluster formation, management and maintenance algorithm, route selection function-based routing

Cite As:

Kumar, K., Kumar, S., Kaiwartya, O., Kashyap, P.K., Lloret, J. and Song, H., 2020. Drone assisted flying ad-hoc networks: mobility and service oriented modeling using neuro-fuzzy. *Ad Hoc Networks*, 106, p.102242.

technique has been suggested for optimized route selection in drone assisted IoT. This technique reduces energy consumption but does not focus on latency and route connectivity.

An Unmanned Aerial Vehicles based emergency rescue framework has been designed for scanning large areas searching through Smartphone signal communication of missing or injured persons [24]. This framework lacks mostly QoS parameters and performance in highly dynamic aerial environment. A new protocol for providing smart communication has been suggested while analyzing sequential patterns of messages with the definition of various fold messages inside UAVs [25]. This protocol reduces energy consumption but does not consider QoS parameters such as delay and route stability. A swarm intelligence-based localization and clustering techniques have been proposed to facilitate communication in emergency inside UAV enabled IoT networks [26]. Firstly proposed, swarm intelligence-based localization is a particle swarm optimization (PSO) based three-dimensional technique while utilizing bounding box algorithm to exploit in 3D search space. Secondly proposed, a swarm intelligence-based clustering is PSO based energy efficient technique which derive fitness function for residual energy, geographic location, inter cluster and intra cluster distance. This technique minimizes computational cost, energy consumption, but does not improve link stability.

## 2.2 QoS- aware routing

Link availability estimation-based routing has been proposed while utilizing the link availability parameter for the selection and updates of a route [27]. Firstly, semi- Markov mobility model has been presented to imitate the behavior of airliners, then link availability period, pdf of relative speed between two aircrafts and expected link lifetime have been used to select the reliable route. In this scheme, relative speed of the derivation for link availability metric and pdf of the link lifetime have been utilized to select reliable route. Still metric of load balance has not been comprised. A joint internet gateway allocation, scheduling and routing scheme has been suggested to minimize the average packet delay in mobile aeronautical ad-hoc networks [28]. Inside it, a mathematical programming scheme has been proposed, while comprising two steps: weighted hop count minimization for scheduling and average delay reduction for routing. Further a genetic algorithm has also been formulated to reduce computational complexity in large mobile network. But this scheme does not provide optimized link lifetime.

A routing and scheduling technique based on hybrid genetic approach has been proposed while supporting the communication among ground vehicle and multiple drones for efficient delivery of parcels [29]. Further hybrid genetic approach consists of population initialization, low visit cost crossover algorithm and three hierarchical education algorithms for fair distribution inside population while avoiding premature convergence and minimizing the total delay. But this technique does not provide optimized link lifetime. Two multi-trip vehicle routing problems have been suggested for drone delivery to minimize the delivery time related to budget constraint [30]. A model for energy consumption has been derived and validated while considering payload and battery weight. The other QoS parameters such as link availability, jitter etc. have not been considered. A vehicle assisted multi-drone scheduling and routing technique has been proposed while optimizing anchor point selection, tour assignment and route planning in each iteration [31]. This technique minimizes total finish time but does not consider residual route load capacity and route availability. A traffic load balancing technique has been suggested to minimize latency for drone-based fog network inside IoT [32]. Two algorithms: heuristic and user association have been utilized sequentially, to solve the traffic load balancing problem.

A motion driven packet forwarding scheme has been suggested in micro aerial vehicle networks while utilizing two predictive heuristics to integrate delay tolerant routing and location aware end-to-end routing [33]. This technique focuses on link connectivity and route delay but does not consider load balancing and energy efficiency. A multi-UAV routing technique has been proposed to solve the multi-UAV coverage task to launch the UAVs while utilizing minimum number of vehicles with minimum delay [34]. This technique reduces the mission time but lacks the other QoS matrices. A jamming-resilient multipath (JaRM) routing technique has been suggested while considering the three major routing matrices: link quality, traffic load and spatial distance in drone based flying ad

Cite As:

Kumar, K., Kumar, S., Kaiwartya, O., Kashyap, P.K., Lloret, J. and Song, H., 2020. Drone assisted flying ad-hoc networks: mobility and service oriented modeling using neuro-fuzzy. *Ad Hoc Networks*, 106, p.102242.

hoc networks [35]. Enhanced link quality and light traffic load are positive factors of this technique, but this technique does not minimize the route latency. A deep reinforcement learning based solution for 3D continuous movement control of multiple drones has been suggested to maximize the energy efficiency and connectivity of drone network [36]. Furthermore, based on coverage fairness, QoS requirements and energy utilization inside drone networks, a reward function has been formulated. The penalty for disconnected drone networks has been introduced while reducing the reward function value drastically. This technique only works in centralized ad-hoc network not in decentralized network [37-40]. A bio-inspired technique based on swarm intelligence has been proposed to control the network topology and to support multimedia traffic for emergency inside FANET [41]. This technique does minimize the route delay.

Table 1 Notations

Notation	Description	Notation	Description
$v^\alpha$	Target velocity	$c^k$	Load capacity of node k
$\emptyset^\alpha$	Horizontal direction	$C^i$	Load capacity of route i
$v''$	Relative velocity	$C^{max}$	Max route load capacity
$v^m$	Velocity vector of node	$D^i$	Total delay of route i
$E(T)$	Expected link availability period	$L$	Availability factor
$L^i$	Availability factor of route i	$C$	Residual load capacity
X	Sender's X coordinate	D	Delay
Y	Sender's Y coordinate	$T^s$	Time stamp
V	Sender's velocity	$B^{id}$	Broadcast ID

### 3. QoS provisioning Drone Communication (D-IoT)

In this section, the proposed drone assisted distributed routing framework focusing on quality of service provision is presented in detail. Firstly, a network model comprising mobility model of drone in flying adhoc networks is discussed. Secondly, QoS metrics: route availability factor, residual route load capacity and route delay are formulated. Hence, route selection approach based on QoS metrics, and broadcast optimization technique have been described. It is highlighted that the mathematical modeling presented as network model and metrics derivations for drone centric network environment is further realized as a complete information routing framework utilizing neuro fuzzy technique. Moreover, it is highlighted that this proposal focuses on drone centric dynamic network environment where parameters such as link quality, route availability, delay, residual energy have significant impact on network performance modelling. Therefore, we have focused in-depth mathematical modelling of the parameters utilizing highly scientific probabilistic modelling approach.

#### 3.1 Drone Network mobility model

The network model consists of three components: drone, ground stations and drone controller station. Here ground stations work as Internet gateways (IGs). This scenario concerns only about the communication between drone and IGs, not satellite based communication. For simplification, some



Cite As:

Kumar, K., Kumar, S., Kaiwartya, O., Kashyap, P.K., Lloret, J. and Song, H., 2020. Drone assisted flying ad-hoc networks: mobility and service oriented modeling using neuro-fuzzy. *Ad Hoc Networks*, 106, p.102242.

assumptions have been considered. The distribution of all drones is done in a plane. Physical layer, transmission power and transmission range related to all drones are uniform. Automatic dependent surveillance-broadcast(ADS-B) system is being equipped for all drones to acquire real-time state vector such as position, velocity, ID and other information.

On the basis of airliner's mobile trace in the sky, we can categorize a drone node movement in to five phases: acceleration phase, steady climb, middle smooth, steady down and deceleration. In the acceleration phase, velocity of drone increases until the target velocity  $v^\alpha$ . Drone selects targeted horizontal direction  $\emptyset^\alpha$  in the range  $[0, 2\pi]$ . In the steady climb phase, drone climbs in the target vertical direction  $\emptyset^\alpha$  in the range  $[0, \pi/2]$  and moves with constant velocity  $v^\alpha$ . Here  $v^\alpha$  is randomly considered in the range 20-50 km/hr and is considered as standard velocity in various drone models. During the middle smooth phase, movement of drone is steady and smooth according to Gauss Markov model [42]. Further in steady down phase, velocity of drone is equal to  $v^\alpha$ . The drone selects horizontal direction equals to  $\emptyset^\alpha$  and vertical direction in the range  $[\pi/2, \pi]$ . In the end, in deceleration phase, drone uniformly decreases the velocity in one direction until it stops. In the starting, in acceleration phase, drone takes 5 min. for takeoff and in the end in deceleration phase, it also takes 5 min. for landing.

### 3.2 Route availability factor

Route availability factor between the non-neighboring drones, is defined as the minimum link availability factor between intermediate nodes in the present route. Link availability factor is the measure of link reliability based on the expected link availability period. Assuming, drone nodes  $M$  and  $N$  are two intermediate nodes and these drones lie in the transmission range of each other.

#### 3.2.1 Probability density function of relative velocity

Let  $\mathbf{v}_m$  and  $\mathbf{v}_n$  are velocity vectors of two drone nodes  $M$  and  $N$  and  $\mathbf{v}_r$  is relative velocity between them. According to fig.2,  $\alpha$  is the angle between two nodes and uniformly distributed between  $[0, \pi]$ . Let  $v_m$ ,  $v_n$  and  $v_r$  are modulus of vectors  $\mathbf{v}_m$ ,  $\mathbf{v}_n$  and  $\mathbf{v}_r$ . According to cosine theorem,

$$v_r = \sqrt{v_m^2 + v_n^2 - 2v_m v_n \cos \alpha} \quad (1)$$

Since  $v_m$ ,  $v_n$  and  $\alpha$  are independent, therefore joint probability density function  $f_{v_m, v_n, \alpha}(v_m, v_n, \alpha)$  can be expressed as

$$f_{v_r}(v_r) = f_{v_m}(v_m) f_{v_n}(v_n) f_\alpha(\alpha) \quad (2)$$

where  $f_{v_m}(v_m)$ ,  $f_{v_n}(v_n)$ , and  $f_\alpha(\alpha)$  are the probability density functions of  $v_m$ ,  $v_n$  and  $\alpha$  respectively and  $v_m^{min}$ ,  $v_m^{max}$  and  $v_n^{min}$  and  $v_n^{max}$  are minimum and maximum velocities of two drone nodes  $M$  and  $N$ . For simplicity, we assume  $v_m = v_n = v$ . The joint pdf  $f_{v_m, v_n, \alpha}(v_m, v_n, \alpha)$  can be written as

$$f_{v_r}(v_r) = f_v^2(v) f_\alpha(\alpha) \quad (3)$$

Now probability density function  $f_\alpha(\alpha)$  can be calculated as

$$f_\alpha(\alpha) = k_1 \sqrt{2v} \sqrt{1 - \cos \alpha} \quad (4)$$

Where  $k_1 \sqrt{2v} \int_0^\pi \sqrt{1 - \cos \alpha} d\alpha = 1$ , on solving, we get  $k_1 = 1/4v$ . Similarly, the probability density function  $f_v(v)$  can be calculated as

$$f_v(v) = k_2 \sqrt{2} \sqrt{1 - \cos \alpha} v \quad (5)$$

Where  $k_2 \sqrt{2} \sqrt{1 - \cos \alpha} \int_{(v^{min})^2}^{(v^{max})^2} v dv = 1$ ,

we get  $k_2 = \sqrt{2} / \sqrt{1 - \cos \alpha} ((v^{max})^2 - (v^{min})^2)$ .

Cite As:

Kumar, K., Kumar, S., Kaiwartya, O., Kashyap, P.K., Lloret, J. and Song, H., 2020. Drone assisted flying ad-hoc networks: mobility and service oriented modeling using neuro-fuzzy. *Ad Hoc Networks*, 106, p.102242.

Therefore, the probability density function  $f_{v,\alpha}(v, \alpha)$  can be expressed as

$$f_{v_r}(v_r) = f_{v,\alpha}(v, \alpha) = \frac{v^2 \sqrt{2-2 \cos \alpha}}{((v^{max})^2 - (v^{min})^2)^2} \quad (6)$$

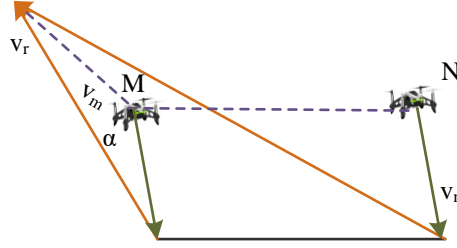


Fig.2. Analysis for the relative velocity of two drones

It is highlighted that the mathematical derivations presented are highly significant for in-depth scientific basis for each of the conceptual idea in the manuscript. This mathematical basis has more value in highly dynamic drone framework implementation environment, where network communication probability depends on metrics such as link availability, residual energy, delay, etc. Therefore, the modeling derivation of these parameters mathematically verifies the validity of our conceptual framework for drones. Further, to calculate the probability density function  $f_{v,\alpha}(v, \alpha)$  of relative velocity ( $v_r$ ) between two drone nodes, we need to calculate the probability density function  $f_\alpha(\alpha)$  and  $f_v(v)$  separately. Therefore, in Eq. (4), probability density function  $f_\alpha(\alpha)$  has been calculated. Here,  $\alpha$  is the angle between two drone nodes and uniformly distributed between  $[0, \pi]$ . Therefore, following probability density function  $f_\alpha(\alpha)$  is calculated as given in Eq. (4) by following uniformly distributed variable formulation.

### 3.2.2 Expected link availability period

Here first derivation for cumulative distribution function for link availability period between neighboring drone nodes is estimated. Then expected link availability period is formulated. Assuming starting distance vector between drone nodes M and N lies in y-axis direction and  $d_0$  is starting distance value. The starting relative velocity vector between nodes M and N is shown in fig.3 We assume angle between initial distance vector and initial relative velocity vector is  $\emptyset$  distributed in uniform manner ranging from 0 to  $\pi$ . Link distance of two neighboring drone nodes, M and N is formulated as follows

$$d_m = d_0 \cos \emptyset + \sqrt{K^2 - d_0^2 \sin^2 \emptyset} \quad (7)$$

Then PDF of link distance of two neighboring drone nodes, M and N is formulated as follows

$$f_{d_m}(d_m) = f_{d_0}(d_0) f_\emptyset(\emptyset) \quad (8)$$

PDF of  $\emptyset$  is expressed as

$$f_\emptyset(\emptyset) = \frac{1}{\pi} \quad (9)$$

PDF of  $d_0$  can be calculated as

$$f_{d_0}(d_0) = h(d_0 \cos \emptyset + \sqrt{K^2 - d_0^2 \sin^2 \emptyset}) \quad (10)$$

Cite As:

Kumar, K., Kumar, S., Kaiwartya, O., Kashyap, P.K., Lloret, J. and Song, H., 2020. Drone assisted flying ad-hoc networks: mobility and service oriented modeling using neuro-fuzzy. *Ad Hoc Networks*, 106, p.102242.

Where,  $\int_{d_{\min}}^{d_{\max}} h(d_0 \cos \phi + \sqrt{K^2 - d_0^2 \sin^2 \phi}) d d_0 = 1$

On solving, we get 
$$h = \frac{6d_{\max} \sin^2 \phi}{3d_{\max}^2 \cos \phi - 2(k^2 - d_{\max}^2 \sin^2 \phi)^{3/2}} - \frac{6d_{\min} \sin^2 \phi}{3d_{\min}^2 \cos \phi - 2(k^2 - d_{\min}^2 \sin^2 \phi)^{3/2}}$$

Then PDF  $f_{d_m}(d_m)$  can be expressed as

$$f_{d_m}(d_m) = \frac{d_0 \cos \phi + \sqrt{K^2 - d_0^2 \sin^2 \phi}}{\pi} \left( \frac{6d_{\max} \sin^2 \phi}{3d_{\max}^2 \cos \phi - 2(k^2 - d_{\max}^2 \sin^2 \phi)^{3/2}} - \frac{6d_{\min} \sin^2 \phi}{3d_{\min}^2 \cos \phi - 2(k^2 - d_{\min}^2 \sin^2 \phi)^{3/2}} \right) \quad (11)$$

Link availability period  $t$  between nodes  $M$  and  $N$  is expressed as

$$t = \frac{d_m}{v_r} \quad (12)$$

Using Eq. 7 to 12, PDF of link availability period between nodes  $M$  and  $N$  is expressed as

$$\begin{aligned} f^T(t) &= \int_0^{v_{\max}} v_r f_{d_m v_r}(v_r t, v_r) dv_r \\ &= \int_0^{v_{\max}} v_r [f_{d_m}(d_m)]_{d_m=v_r t} \left[ \frac{v^2 \sqrt{2-2 \cos \alpha}}{((v_{\max})^2 - (v_{\min})^2)^2} \right] dv_r \end{aligned} \quad (13)$$

Then expected link availability period is estimated as

$$E(T) = \int_0^\infty t f^T(t) dt \quad (14)$$

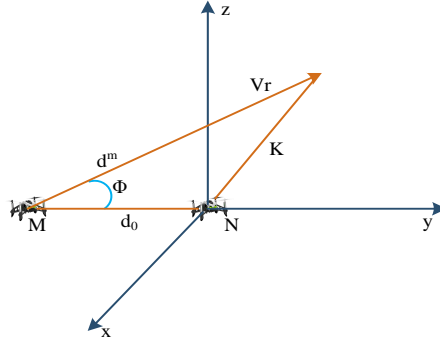


Fig.3. Link availability period between drone nodes M and N

### 3.2.3 Route availability factor calculation

Link availability period between nodes  $M$  and  $N$  is expressed as follows from fig.3

$$T^{MN} = \frac{d_0 \cos \phi + \sqrt{K^2 - d_0^2 \sin^2 \phi}}{v''} \quad (15)$$

Link availability factor between nodes  $M$  and  $N$  is formulated as

$$L^{MN} = \min \left( \frac{T^{MN}}{E(T)}, 1 \right) \quad (16)$$

Let  $L^i$  is the route availability factor of route  $i$ , then  $L^i$  is estimated as

$$L^i = \min \{L^{MN}\} \quad (17)$$



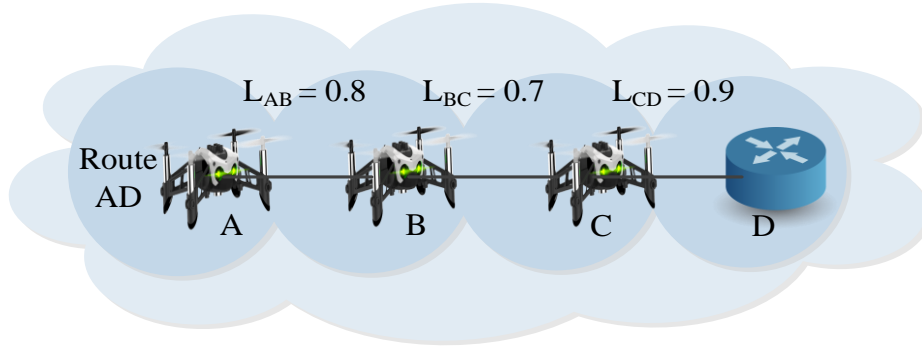


Fig.4. Route availability factor calculation

According to fig.4, link availability factor which is minimum in this route has been considered as the route availability factor of the route AD. That is to say

$$L^{AD} = L^{BC} = 0.7 .$$

### 3.3 Residual Route load capacity

In In this section, residual load capacity of route between two nodes is formulated. Residual route load capacity is defined as the minimum residual load capacity amongst all node's residual load capacity along the route. Assuming,  $c^k$  is the residual load capacity for drone node  $k$ . Hence  $c^k$  is expressed as

$$c^k = \delta - \sum_{k=1}^m \omega_k l_k \quad (18)$$

Where,  $\delta$  is the maximum load capacity for drone node  $k$ , while  $l_k$  and  $\omega_k$  are the average packet size related to traffic and average packet arrival rate of  $m$  sources, respectively. Let  $C^i$  be the residual load capacity for route  $i$ , the  $C^i$  is formulated as

$$C^i = \min \{c^k\} \quad (19)$$

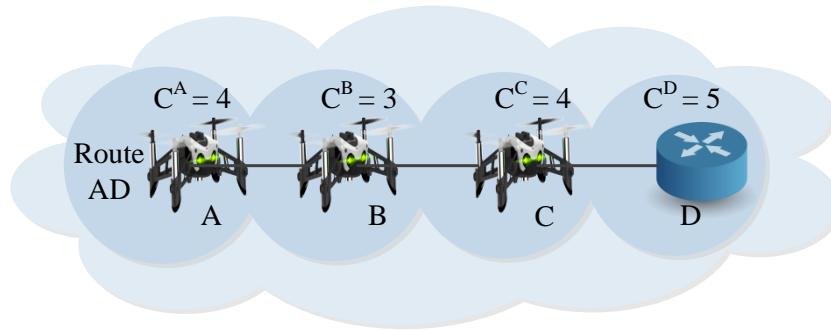


Fig.5. Residual route load capacity calculation

In this protocol, route having minimum residual load capacity is prefer in route finding process. Fig.5 shows the calculation process for residual load capacity for route AD, where residual load capacity of node B having minimum residual load capacity equals to 3 is the residual load capacity of route AD.

### 3.4 Route Delay

Cite As:

Kumar, K., Kumar, S., Kaiwartya, O., Kashyap, P.K., Lloret, J. and Song, H., 2020. Drone assisted flying ad-hoc networks: mobility and service oriented modeling using neuro-fuzzy. *Ad Hoc Networks*, 106, p.102242.

Route delay is defined as the time required to send a data packet from source drone node to destination drone node. Usually route delay mainly comprises queuing delay, propagation delay and transmission delay based on scheduling techniques, traffic control schemes of nodes, residual link bandwidth, processing power of ports and traffic characteristics. Here leaky bucket control strategy as illustrates in fig.6 is utilized to control communication volume of drones. Assuming  $\lambda$  is the bucket capacity,  $\mu_{in}$  is the input flow rate and  $\mu_{out}$  is the service rate. As service rate at each drone varies, so highest data flow of link is dependent on the drone node which has least service rate, therefore

$$\mu_{out} = \min \{ \mu_{out}^1, \mu_{out}^2, \mu_{out}^3, \dots, \mu_{out}^n \}$$

If  $d$  is the queuing delay then according to the leaky bucket strategy,

$$\lambda + \mu_{in}d < \mu_{out}d \quad (20)$$

hence

$$d = \frac{\lambda}{\mu_{out} - \mu_{in}} \quad (21)$$

For the links,  $\lambda = \rho - nS^{max}$  where  $\rho$  is sudden traffic depended on the network and  $S^{max}$  represents maximum packet size, then queuing delay is expressed as

$$d = \frac{\rho - nS^{max}}{\mu_{out} - \mu_{in}} \quad (22)$$

Let  $D^i$  is the total delay of route  $i$ , and  $B_j$  and  $p_j$  are bandwidth and propagation delay of link  $j$  respectively. The route delay can be expressed as

$$D^i = \frac{\rho - nS^{max}}{\mu_{out} - \mu_{in}} + \sum_{j=1}^n \frac{S^{max}}{B_j} + \sum_{j=1}^n p_j \quad (23)$$

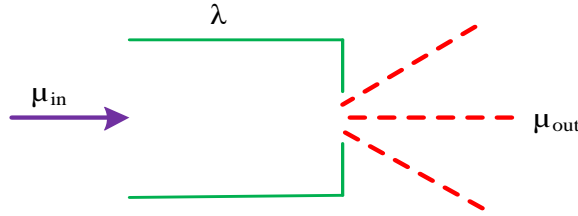


Fig.6. Leaky bucket strategy

### 3.5 Single metric

Initially, In D-IoT, all the QoS metrics: route availability factor, residual route load capacity, and route delay are jointly considered for the purpose of finding the optimized route. Let  $P^k$  is considered as the single metric for route  $k$ . The metric  $P^k$  is evaluated by employing a neuro-fuzzy inference system (NFIS). It is far better than fuzzy logic inference system because of unlike another artificial neural network, NFIS have higher capability to adapt an environment's requirement in the learning process and adjust the weight of membership function of fuzzy logic inference system and reduces the error rate in determining the rules in fuzzy logic [43]. It is a feed-forward adaptive neural network which uses supervised learning algorithm for learning process. NFIS follows the learning process of Takagi-Sugeno fuzzy inference system [44]. The basic architecture of NFIS with three input parameter route availability factor (L), residual route load capacity (C), route delay (D) and one output single metric (P) are shown in fig 7.

Each of these three input parameters have three membership functions, according to Takagi- Sugeno fuzzy inference model that contains 27 rules. NFIS consists of five layers architecture; Fuzzy layer, T-norm layer, normalized layer, de-fuzzy layer and aggregated layer. The first fuzzy layer (as known

Cite As:

Kumar, K., Kumar, S., Kaiwartya, O., Kashyap, P.K., Lloret, J. and Song, H., 2020. Drone assisted flying ad-hoc networks: mobility and service oriented modeling using neuro-fuzzy. *Ad Hoc Networks*, 106, p.102242.

as membership/antecedent layer) and fourth de-fuzzy layer (consequent layer) are adaptive in nature because they are updated according to results obtained and rest of the layers are non-adaptive in nature.

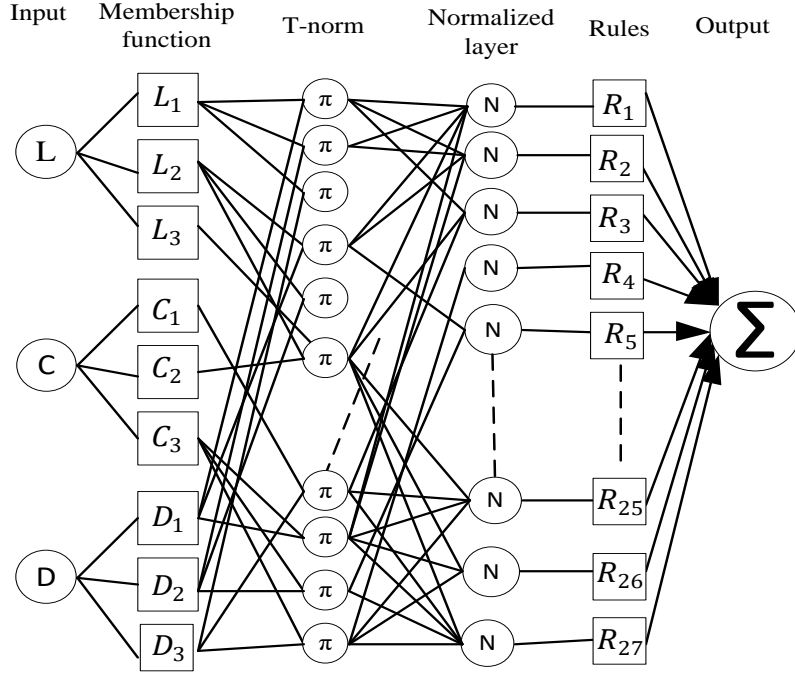


Fig. 7. NFIS with 3-input, 27 rules and one output

Table 2 Fuzzy rules database

Rule	IF			THEN	Rule	IF			THEN
	L	C	D	P		L	C	D	P
1.	$L_1$	$C_1$	$D_1$	$P_3$	15.	$L_2$	$C_2$	$D_3$	$P_3$
2.	$L_1$	$C_1$	$D_2$	$P_3$	16.	$L_2$	$C_3$	$D_1$	$P_2$
3.	$L_1$	$C_1$	$D_3$	$P_1$	17.	$L_2$	$C_3$	$D_2$	$P_1$
4.	$L_1$	$C_2$	$D_1$	$P_2$	18.	$L_2$	$C_3$	$D_3$	$P_1$
5.	$L_1$	$C_2$	$D_2$	$P_3$	19.	$L_3$	$C_1$	$D_1$	$P_7$
6.	$L_1$	$C_2$	$D_3$	$P_1$	20.	$L_3$	$C_1$	$D_2$	$P_6$
7.	$L_1$	$C_3$	$D_1$	$P_2$	21.	$L_3$	$C_1$	$D_3$	$P_5$
8.	$L_1$	$C_3$	$D_2$	$P_2$	22.	$L_3$	$C_2$	$D_1$	$P_5$
9.	$L_1$	$C_3$	$D_3$	$P_1$	23.	$L_3$	$C_2$	$D_2$	$P_3$
10.	$L_2$	$C_1$	$D_1$	$P_4$	24.	$L_3$	$C_2$	$D_3$	$P_3$
11.	$L_2$	$C_1$	$D_2$	$P_3$	25.	$L_3$	$C_3$	$D_1$	$P_2$
12.	$L_2$	$C_1$	$D_3$	$P_2$	26.	$L_3$	$C_3$	$D_2$	$P_1$
13.	$L_2$	$C_2$	$D_1$	$P_4$	27.	$L_3$	$C_3$	$D_3$	$P_1$
14.	$L_2$	$C_2$	$D_2$	$P_3$					

The linguistic variables for three input parameters are given as follows: route availability factor (L) = {below, good, top} and is denoted by  $\{L_1, L_2, L_3\}$ , residual route load capacity (C) = {min, avg, max} that is denoted by  $\{C_1, C_2, C_3\}$ , route delay (D) = {low, medium, high} as  $\{D_1, D_2, D_3\}$  and output single metric ( $P^k$ ) = {weakest, weaker, weak, medium, strong, stronger, strongest} as  $\{P_1, P_2, P_3, P_4, P_5, P_6, P_7\}$ . The first layer's membership nodes follow the rules influenced by If-Then rules as shown in table -2. The antecedent parts of rules in the table-1 represent the input fuzzy subspace and consequent part of rule in the table shows the output inside the fuzzy subspace. We

Cite As:

Kumar, K., Kumar, S., Kaiwartya, O., Kashyap, P.K., Lloret, J. and Song, H., 2020. Drone assisted flying ad-hoc networks: mobility and service oriented modeling using neuro-fuzzy. *Ad Hoc Networks*, 106, p.102242.

developed for three input parameters with three linguistic variables ( $3^3$ ) 27 If-Then rules for the proposed NFIS architecture governed by Takagi-Sugeno fuzzy inference system. The rules can be expressed as

Rule 1 = If L is  $L_1$ , C is  $C_1$  and D is  $D_1$  Then  $P_1 = q_1L + r_1C + s_1D + t_1$

Rule 2 = If L is  $L_1$ , C is  $C_1$  and D is  $D_2$  Then  $P_2 = q_2L + r_2C + s_2D + t_2$

Rule 3 = If L is  $L_1$ , C is  $C_1$  and D is  $D_3$  Then  $P_3 = q_3L + r_3C + s_3D + t_3$

Rule 4 = If L is  $L_1$ , C is  $C_2$  and D is  $D_1$  Then  $P_4 = q_4L + r_4C + s_4D + t_4$

.

.

Rule 25 = If L is  $L_3$ , C is  $C_3$  and D is  $D_1$  Then  $P_{25} = q_{25}L + r_{25}C + s_{25}D + t_{25}$

Rule 26 = If L is  $L_3$ , C is  $C_3$  and D is  $D_2$  Then  $P_{26} = q_{26}L + r_{26}C + s_{26}D + t_{26}$

Rule 27 = If L is  $L_3$ , C is  $C_3$  and D is  $D_3$  Then  $P_{27} = q_{27}L + r_{27}C + s_{27}D + t_{27}$

Where  $L_1, C_1, D_1$  are membership function of input parameter antecedent (If) part, while  $q_1, r_1, s_1$  and  $t_1$  are linear parameters of consequent (then) part of Takagi-Sugeno model. The operation of NFIS to select single metric output  $P^k$  describe by layer wise as follows.

- 1) **Fuzzy Layer**- the nodes in this layer are represented by square, which are adaptable in nature during backward pass. Each node resembles to membership function of input parameters. The output of this layer is degree of membership govern by input membership function in the range of 0 and 1. The membership function can be triangular, trapezoidal, Gaussian, and generalized bell membership function. In this work, we considered Gaussian (Eq. 24) and generalized bell membership function (Eq. 25).

$$\mu_{L\alpha}(L) = \exp\left[-\left(\frac{L-z_\alpha}{2x_\alpha}\right)^2\right] \quad (24)$$

$$\mu_{L\alpha}(L) = \frac{1}{1 + \left|\frac{m-z_\alpha}{x_\alpha}\right|^{2y}} \quad (25)$$

The output of first layer is given by

$$\begin{aligned} O_{1,\alpha} &= \mu_{L\alpha}(L), & \alpha &= 1,2,3 \\ O_{1,\alpha} &= \mu_{C\alpha}(C), & \alpha &= 1,2,3 \end{aligned}$$

$$O_{1,\alpha} = \mu_{D\alpha}(D), \quad \alpha = 1,2,3$$

Where  $\mu_{M\alpha}, \mu_{N\alpha}$  and  $\mu_{O\alpha}$  are membership functions of adaptive node  $L, C$  and  $D$  respectively and  $x_\alpha, y_\alpha$  and  $z_\alpha$  are premises parameters of membership functions that are responsible for customize the shape of membership functions. The membership function  $O_{1,\alpha}$  represents the degree to which L satisfies the input parameter  $L_\alpha$ .

- 2) **T-Norm Layer**- this layer determines the firing strength of each rule associated with input signals. All the nodes in this layer are non-adaptive in nature and are depicted by circle with labeled  $\pi$ . The output of T-norm (rule) layer evaluated as multiplying all the incoming signals to node and delivered output to the next layer nodes. The T-Norm layer applies generic AND operator to multiply all the input signals to evaluate the firing strength of rules and generates output  $O_{2\alpha}(T_\alpha)$  as follows.

$$O_{2\alpha} = T_\alpha = \mu_{L\alpha}(L) * \mu_{C\alpha}(C) * \mu_{D\alpha}(D), \quad \alpha = 1,2,3$$

$$O_{2\alpha} = T_\alpha = \mu_{L\alpha}(L) \wedge \mu_{C\alpha}(C) \wedge \mu_{D\alpha}(D), \quad \alpha = 1,2,3 \quad (26)$$

- 3) **Normalized layer**- The firing strength of each rule is normalized corresponding to summation of all rules firing strength. The nature of node in this layer is also non-adaptive and labeled with N within circle. The normalized firing strength of rule can be expressed the output  $O_{3\alpha}$  as follows.

$$O_{3\alpha} = T_{n\alpha} = \frac{T_\alpha}{\sum_\alpha T_\alpha}, \quad \alpha = 1,2,3 \quad (27)$$

- 4) **Defuzzy Layer**- Nodes in this layer are adaptive in nature and labeled with R within square. The output of adaptive node is the multiplication of normalized firing strength of rule and premises

Cite As:

Kumar, K., Kumar, S., Kaiwartya, O., Kashyap, P.K., Lloret, J. and Song, H., 2020. Drone assisted flying ad-hoc networks: mobility and service oriented modeling using neuro-fuzzy. *Ad Hoc Networks*, 106, p.102242.

parameter of input parameter. The output is also known as consequent parameter and can be expressed as

$$O_{4\alpha} = T_{n\alpha} P_{\alpha} = T_{n\alpha} (q_{\alpha}L + r_{\alpha}C + s_{\alpha}D + t_{\alpha}) \quad (28)$$

Where  $T_{n\alpha}$  normalized firing strength of rule is obtained from previous (third layer) and  $P_{\alpha}$  is premises parameter of the node.

- 5) **Aggregated Output layer**- Non-adaptive nature of single node is used to estimate the output, which measures the overall system performance. The output is the summation of all the incoming signals to this layer, labeled as  $\sum$  inside the circle to represent the aggregated output.

$$O_{5\alpha} = P^k = \sum_{\alpha} T_{n\alpha} P_{\alpha} = \frac{\sum_{\alpha} T_{n\alpha} P_{\alpha}}{\sum_{\alpha} T_{n\alpha}} \quad (29)$$

A neuro-fuzzy selection algorithm (Algorithm-1) is presented to describe the process of NFIS. NFIS uses hybrid learning algorithm based on gradient descent and least mean square to train the membership function of input parameter worked on two passes: forward pass and backward pass. The first layer and fourth layer node are updated over time. In forward pass (training dataset), the input signals (premise parameter {L, D, C}) are fixed in nature and propagated from first layer (as step-6) till to fourth layer (step 11) of proposed Algorithm-1. In the step -7 Gaussian and bell-shaped membership function for each input parameter {L, D, C} are obtained using Eq. (24) and Eq. (25). After that in step -8 using if-then rules and minimum operator AND is applied to customize the firing strength (it defined how much powerful the signal) of each input parameter. Further, firing strength of each input node regarding membership function is normalized with respect to the total firing strength. The output of fourth layer is obtained as aggregated output  $P^k$  using Eq. (29) in step-11 term as consequent parameter. The obtained output is compared with actual output and error is recorded. The primary goal of the ANFIS algorithm is to minimized mean square error ( $|\text{obtained output} - \text{actual output}|^2$ ) recursively. While in the backward pass, error occurred in forward pass is sent back to input (first) layer and at the same time membership function of input premises are updated using learning process of gradient descent method. The hybrid learning process (combination of forward pass and backward pass) of one level is known as epoch. The algorithm runs for until convergence (error between actual output and calculated output is infinitesimal small) or maximum number of epochs ( $E_{max}$ ).

---

**Algorithm 1: Neuro-fuzzy Selection Algorithm (NFSA)**

---

**Input:** L, D, C and  $E_{max}$ ;

**Process:**

1. **For** E=1 to  $E_{max}$ .
  2. Input the nonlinear premises into first layer of Takagi- Sugeno inference engine.
  3. Produce the parameter Membership function  $\mu_{L\alpha}(L)$  for each node according to Eq. (24) and (25) in adaptive Fuzzy layer.
  4. Customize the firing strength of each node ( $T_{\alpha}$ ) according to Eq. (26) in T-norm layer
  5. Normalize the firing strength of each node ( $T_{n\alpha}$ ) according to Eq. (27) in normalized layer.
  6. Update the consequent parameter of each node using Eq. (28) in Adaptive Defuzzification layer.
  7. Produce the aggregated output  $P^k$  for overall system according to Eq. (29).
  8. **Output:**  $P^k$
- 

Packet. Type	Source. Address	Destination Address	Location	Velocity	L <sup>GAD</sup>	C <sup>GAD</sup>	D <sup>GAD</sup>	Broadcast ID
-----------------	--------------------	------------------------	----------	----------	------------------	------------------	------------------	-----------------

Fig. 8. Structure of IG advertisements (IGAD) message

### 3.6 Best advertisement-based forwarding (BADF) technique

Cite As:

Kumar, K., Kumar, S., Kaiwartya, O., Kashyap, P.K., Lloret, J. and Song, H., 2020. Drone assisted flying ad-hoc networks: mobility and service oriented modeling using neuro-fuzzy. *Ad Hoc Networks*, 106, p.102242.

In this section, best advertisement-based forwarding (BADF) technique is discussed, with the involvement of three aspects for controlling the overhead related to advertisement flooding. Firstly, the IP address of originator, and broadcast ID of previously received IG advertisements (IGADs), and newly received IGADs are checked by a drone. If drone finds duplicate IGADs, having similar IP address of originator, broadcast ID of previously received and newly received IGAD, then the duplicate IGADs are discarded by this drone. Hence, the congestion caused by duplicate IGADs is avoided based on the advertisement flooding in the network.

Secondly, the drones not yet taken off or already landed (having zero velocity) discard all the received IG advertisements. These drones are not involved during routing table computation. Therefore, this results in the form of limited broadcasting and reduction in network congestion.

In the last, a drone rebroadcasts the IGADs with route availability factor and residual route load capacity, higher as compared to threshold value and route delay lower than threshold value. Hop count between drone node and IG should be lower as compared to maximum hop count. Hence, this minimizes the traffic overhead caused by broadcasting advertisement.

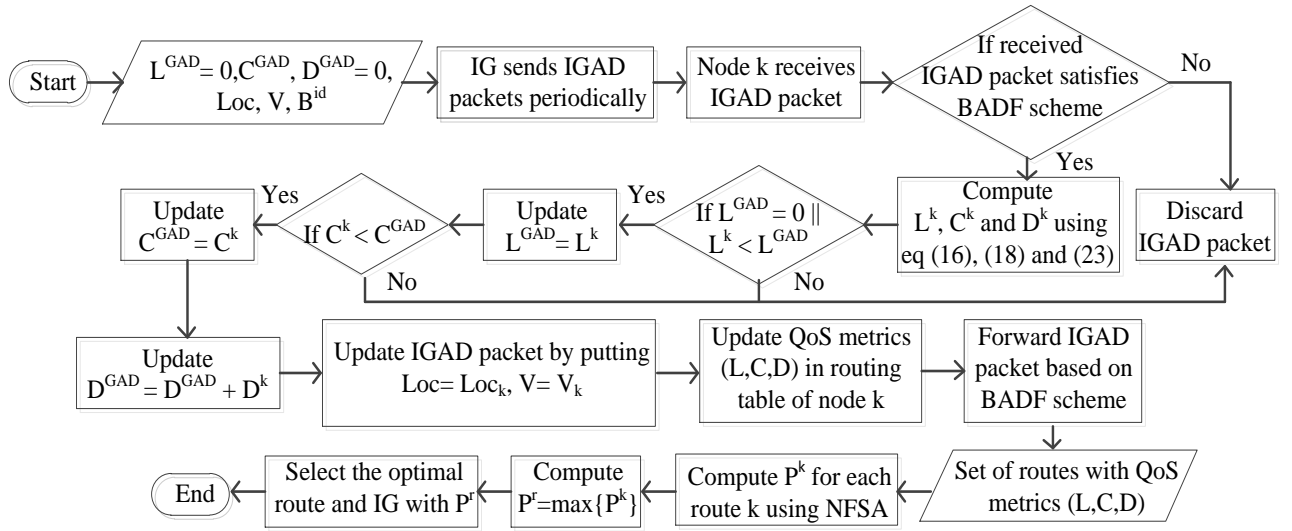


Fig.9. Optimal route and IG selection process of D-IoT

### 3.7 QoS provisioning Drone assisted routing

The In this protocol, IGs broadcast IGADs for advertising their QoS metrics ( $L, C, D$ ) periodically inside the network. Further, drone node knows their information on the basis of IGADs. In this protocol, we assume all IGs have the same IGAD interval. Let IGADs for  $L, C$  and  $D$  are  $L^{GAD}$ ,  $C^{GAD}$  and  $D^{GAD}$ .  $T^s$  is timestamp or time at which packet is sent. The format for IGAD message is illustrated in fig.8.

---

#### Algorithm 2: QoS provisioning Drone assisted routing

---

**Input:**  $Loc, V, L^{GAD} = 0, C^{GAD}, D^{GAD} = 0, B^{id}$ ;

**Process:**

1. IGAD ( $Loc, V, L^{GAD} = 0, C^{GAD}, D^{GAD} = 0, B^{id}$ )
2. IG sends IGADs periodically.
3. Drone node  $k$  receives IGAD packet.
4. **if** received packet based on BADF scheme condition **then**
5.     Node  $k$  computes  $L^k, C^k$  and  $D^k$  according to Eq. (16) and (18) and (23).
6.     **if** ( $L^{GAD} = 0 \parallel L^k < L^{GAD}$ ) **then**
7.          $L^{GAD} = L^k$ .



```

8.      end if
9.      if( $C^k < C^{GAD}$ )then
10.          $C^{GAD} = C^k$ .
11.      end if
12.          $D^{GAD} = D^{GAD} + D^k$ .
13.         Update IGAD packet while replacing,  $Loc$  and  $V$  with  $Loc_k$  and  $V_k$ , and updating  $T^S$ .
14.         Update route QoS metrics ( $L, C, D$ ) in routing table of node  $k$ .
15.         Forward IGAD packet based on BADF scheme
16.      else discard IGAD packet;
17.      end if
18.      Compute  $P^k$  for each route  $k$  using NFSA
19.       $P^r = \max \{P^k\}$ 
20.      Select the route with  $P^r$ 
21.      Select the IG with  $P^r$ 
22.      Output: Optimized route and IG

```

---

After receiving IGAD packet, drone node estimates the values of  $L^k$ ,  $C^k$  and  $D^k$  on the basis of eq. (16), (18) and (23). If the values of  $L^k$  or/and  $C^k$  are lower than the values of  $L^{GAD}$  or/ and  $C^{GAD}$ , then QoS metrics ( $L, C, D$ ) are updated in drone's routing table and location ( $X, Y$ ), velocity  $V$  and  $T^S$  are updated in IGAD packet. Otherwise current  $L^{GAD}$  or/and  $C^{GAD}$  are utilized in the routing table and IGAD also. Further, the value of  $D^{GAD}$  is updated by adding the value of  $D^k$ . Then, on the basis of best advertisement-based forwarding technique IGAD packet is further forwarded inside the network. The basic procedure for route selection is presented by algorithm-II. The message for route updates is sent to the source drone node by the intermediate drone node, if there is possibility of novel link establishment or current link breakage along the route.

In this way, based on updated route parameters, source drone node decides a potential route to transmit packet. The drone node preserves the records of QoS parameters for each route to IGs in the routing table. The optimal route and IG selection process of D-IoT is also presented in Fig.9.

#### 4. Experimental Results and Discussion

In this section, simulation experiments are performed to carry out performance analysis of the proposed Drone assisted distributed routing framework focusing on QoS in IoT environment (D-IoT). Simulations carried out to assess the performance related to the proposed D-IoT framework in drone assisted IoT environment is presented focusing on simulation settings, parameters, and comparative analysis. The implementation of proposal and some state-of-the-art techniques is done using network simulator (ns-2) environment [45]. The major simulation setting includes 200 drones wireless nodes enabled by 802.11b version of Wi-Fi in the simulation area of  $2km \times 2km$ . The wireless transmission range of 200m was considered for Drone-to-Drone and Drone-to-Ground communication with most of computing performed in the ground station server and drones active as service enables in drone assisted IoT environment. The communication link bandwidth between Drone-to-Drone was considered 5Mbps and between Drone-to-Ground server was considered 10Mbps. A total simulation time of 50 minutes was considered for each experiment performed in the simulator. Each data point considered in the experimental results is an average of 10 simulation experiments performed under similar parameter setting to avoid objectivity and bring normalization in result analysis.

Further, it is also clarified that in the simulation 802.11b Wi-Fi was utilized considering its suitability and availability in ns2 network simulation environment. It supports approximately 11Mbps network speed which was enough for the considered network settings in our implementation. For comparative performance analysis, few traditional ad hoc networking framework and a recent drone framework were considered including AODV [16], GPSR [17], and JaRM [35]. Further, range of metrics

Cite As:

Kumar, K., Kumar, S., Kaiwartya, O., Kashyap, P.K., Lloret, J. and Song, H., 2020. Drone assisted flying ad-hoc networks: mobility and service oriented modeling using neuro-fuzzy. *Ad Hoc Networks*, 106, p.102242.

considered in the performance analysis includes packet delivery ratio, number of handoffs among Drones assisted Flying ad hoc networks, overhead and route delay. It is clarified that mathematical modeling derivation in Section 3 are the basis of considering these metrics in the analysis of results. Similar metrics were also considered in recent development in literature on drone assisted FANET environments. However, we have carried out the simulation in ns-2 considering various benefits of the simulation such as basic adhoc protocol support, signal level setting in nodes, freedom of using range of wireless access techniques. We do agree that new simulator support much realistic network environment, and therefore we will plan to work in future in these new simulators. The different color of the protocols represents the level of value of the measure metric. For example, in Fig. 10, the color means the different values of packet deliver ratio. Similarly, in Fig. 12, the color means the different levels of network overhead. A summarized list of major simulation configuration settings is in Table 3.

**Table 3** Simulation setup

Parameters	Values	Parameters	Values
Simulation area	2km $\times$ 2km	MAC protocol	<i>TDMA</i>
Simulation time	50 min	CBR packet size	<i>512 bytes</i>
Trans/Receiv antenna	Omnidirectional	CBR interval	<i>0.01 sec</i>
IGAD interval	Uniform(3.5,4.5) s	Drone-Drone link bandwidth	<i>5 mbps</i>
Drone-Drone trans range	200m	Drone-Ground link bandwidth	<i>10 mbps</i>
Drone-Ground trans range	200m	Packet Type	<i>UDP</i>
Number of drone	200	Channel Type	<i>Wireless</i>
Propagation model	Free space		

#### 4.1 Analysis of Results

Two scenarios: experimental results with same weight factors and experimental results with varying weight factors are considered to analyze the performance of proposed D-IoT with the state-of-the-art protocols.

##### 4.1.1 Analysis of results (with same weight factors)

In this section, experimental results have been described while assigning equal weightage for all the metrics: route availability factor, residual route load capacity, and route delay.

Packet delivery ratio (PDR) is described as the ratio of the number of successfully transmitted packets to the number of total transmitted packets. Fig 10 shows the variation in packet delivery ratio as departure gap of drones and number of drones increase for all the compared protocol: AODV, GPSR, JaRM and D-IoT. According to fig.10, in the starting till threshold value of departure gap (40 min), packet delivery ratio enhances gradually in case of all the compared protocols. But when departure gap increases more than 40 min, then packet delivery ratio reduces for each protocol. D-IoT performs better than the state-of-the-art protocols, for higher departure gap (having  $> 30$  min). In case of AODV and GPSR, overhead increases rapidly, therefore packet delivery ratio reduces quickly after a threshold. While for D-IoT, unstable routes are discarded, therefore packet delivery ratio is higher as compared to AODV, GPSR and JaRM. In case of AODV, GPSR and JaRM, packet delivery ratio decreases gradually when number of drones are 40 or more than 40, but for D-IoT, packet delivery ratio starts decreasing when number of drones are 100. From the fig.10, it is clearly illustrated that

Cite As:

Kumar, K., Kumar, S., Kaiwartya, O., Kashyap, P.K., Lloret, J. and Song, H., 2020. Drone assisted flying ad-hoc networks: mobility and service oriented modeling using neuro-fuzzy. *Ad Hoc Networks*, 106, p.102242.

packet delivery ratio for D-IoT is far higher as compared to state-of-the-art protocols, because D-IoT could select next hop with the shortest queue of packets among all the possible nodes. Thus, this results the avoidance of local blocking.

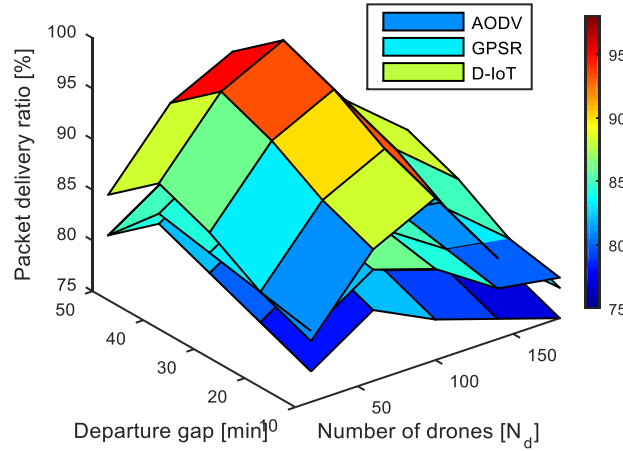


Fig.10.Behavior of PDR with Number of drones and Departure gap

Fig.11 illustrates the impact on packet delivery ratio as traffic load and number of drones vary, while keeping departure gap equals to 25 min. As shown in fig.11, packet delivery ratio decreases as traffic load increases for all the compared protocols. It is clearly enunciated that packet delivery ratio in case of proposed D-IoT is higher than AODV and GPSR because of consideration of route load balancing factor in the proposed D-IoT but not in the state of the arts protocols. In case of D-IoT, packet delivery ratio is higher than packet delivery ratio in case of GPSR, AODV and JaRM, when traffic load varies from 100 kb/s to 500 kb/s.

Overhead is defined as the amount of excess packets generated for the successful delivery of actual number of packets between the source and the destination. Fig.12 illustrates the variation in the overhead as departure gap and quantity of drones increase. As departure gap increases overhead decreases, but when number of drones increase then overhead also increases. Due to utilization of best advertisement-based forwarding scheme to minimize overhead, in case of D-IoT is far lower than AODV and JaRM. But GPSR results less overhead as compared to both D-IoT, JaRM and AODV, because GPSR utilizes smaller periodic hello packet for neighbor discovery as compared to IGAD packet of D-IoT.

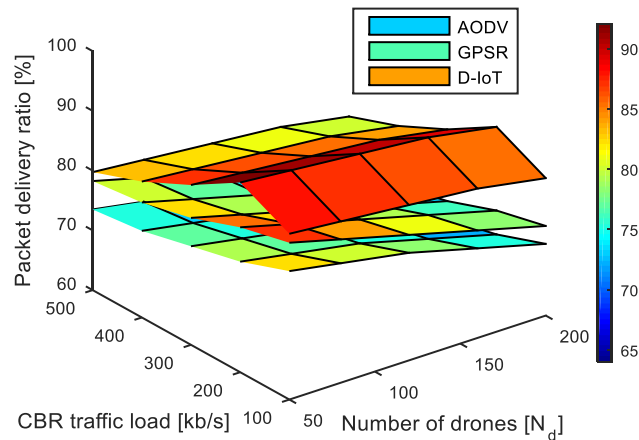


Fig.11.Variation in PDR with Number of drones and Traffic load

Cite As:

Kumar, K., Kumar, S., Kaiwartya, O., Kashyap, P.K., Lloret, J. and Song, H., 2020. Drone assisted flying ad-hoc networks: mobility and service oriented modeling using neuro-fuzzy. *Ad Hoc Networks*, 106, p.102242.

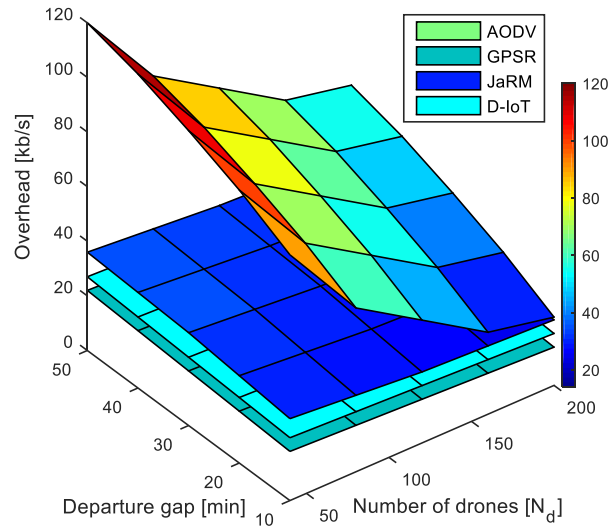


Fig.12.Variation in Overhead with Number of drone and Departure gap

Stability is defined in terms of number of the handoffs, and is inversely proportional to number of handoffs. Fig.13 illustrates the impact of departure gap and number of drones on the average handoffs per hour for all four routing protocols. The performance of D-IoT is better than the state-of-the-art protocols in terms of number of handoffs (stability) because D-IoT comprises better path duration for new route selection. Whereas no path stability metric is considered in case of AODV and GPSR. In terms of average handoffs per hour, JaRM performs better than AODV and GPSR, because path stability metric is utilized in case of JaRM. Still handoff per hour in D-IoT is less than JaRM. The results in fig.13 also show the variation in stability in terms of average number of handoffs when number of drones is considered as 40, 80, 120, 160 and 200. It is clearly enunciated that stability decreases as number of drones increases in case of all the compared protocols. Further with the increment in number of drones, there is slow and less increment in the number of handoffs in case of D-IoT as compared to state-of-the-art protocol. This is because, the more the drones, the larger air communication traffic, and then, D-IoT is more likely to find the next hop more stable with less node delay. As AODV utilizes the hop count as the only metric, and AODV and GPSR both always find the shortest path, which do not comprise link stability. Consequently, drones reach their maximum range in more frequent manner, hence, it is prone to cause handoff.

Route delay is defined as the time required to transmit a data packet from source node to destination node. Fig.14 shows the impact on route delay with the variation in number of drone and CBR traffic load. Route delay in case of D-IoT is lower than GPSR and JaRM because route delay is considered as one of the route selection metrics in D-IoT, but not in GPSR and JaRM. D-IoT also considers local dynamic queue delay for node which avoids the congestion. Whereas, D-IoT has slightly higher route delay as compared to AODV because packets are forwarded through shortest path in case of AODV, but is unstable.

Cite As:

Kumar, K., Kumar, S., Kaiwartya, O., Kashyap, P.K., Lloret, J. and Song, H., 2020. Drone assisted flying ad-hoc networks: mobility and service oriented modeling using neuro-fuzzy. *Ad Hoc Networks*, 106, p.102242.

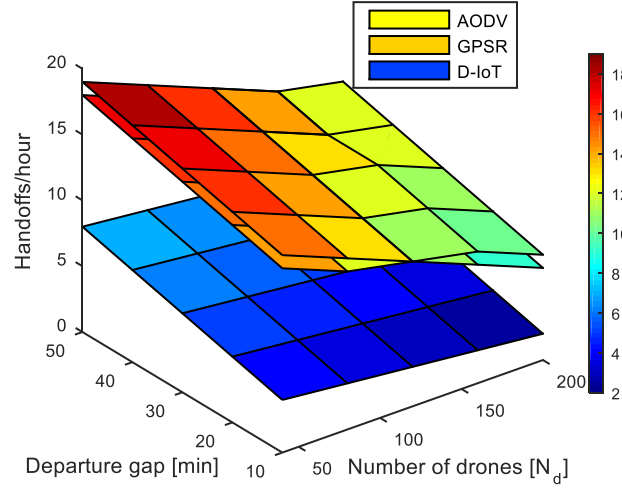


Fig.13. Variation in Handoffs with Number of drones and Departure gap

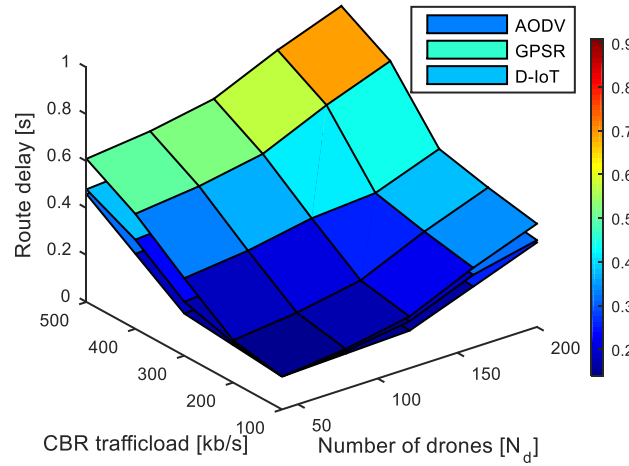


Fig.14. Variation in Route delay with Number of drones and CBR trafficload

#### 4.1.2 Analysis of results (with varying weight factors)

The performance of the proposed D-IoT is optimized while performing the simulation with the consideration of varying weightage corresponding to route metrics according to Neuro-fuzzy system. Three scenarios are presented in simulation for this purpose. In first scenario, the highest priority is given to route availability factor metric, while assigning weight factor: 0.6 for route availability factor metric and weight factor: 0.2 for other metrics equally. The protocol in this scenario is expressed as D-IoT1. In second scenario, the metric: residual route load capacity is prioritized while assigning weight factor: 0.6 for residual route load capacity metric and weight factor: 0.2 for other metrics equally and this scenario is denoted as D-IoT2. In third scenario, the metric: route delay is preferred while assigning weight factor: 0.6 for route delay metric and weight factor: 0.2 for other metrics equally. The protocol in third scenario is expressed as D-IoT3. Further the performance of D-IoT1, D-IoT2 and D-IoT3 are compared with D-IoT0 (without weights), AODV, GPSR and JaRM protocols. A comparison of packet delivery ratio between D-IoT in all scenarios, and the state-of-the-art protocols with varying traffic load and quantity of drones is shown in fig.15. Fig 15(a), 15(b), 15(c)

Cite As:

Kumar, K., Kumar, S., Kaiwartya, O., Kashyap, P.K., Lloret, J. and Song, H., 2020. Drone assisted flying ad-hoc networks: mobility and service oriented modeling using neuro-fuzzy. *Ad Hoc Networks*, 106, p.102242.

and 15(d) shows the comparison between packet delivery ratio and traffic load, when number of drones are considered as 40,80,120 and 200. As shown in all scenarios of fig 15, packet delivery ratio is increasing until number of drones are 80 and then decreasing when number of drones are increased in case of all protocols. It is also illustrated that packet delivery ratio is lesser and decreasing rapidly in case of AODV and GPSR, as compared to packet delivery ratio in D-IoT0, D-IoT1, D-IoT2 and D-IoT3. But in case of JaRM, packet delivery ratio is higher and decreasing slowly as compared to packet delivery ratio for AODV and GPSR, but lesser than packet delivery ratio in case of all scenarios of D-IoT. packet delivery ratio in case of D-IoT3 is lesser than rest scenarios of D-IoT, because of more consideration of route delay as compared to route availability factor and residual route load capacity. D-IoT0, D-IoT1, D-IoT2 and D-IoT3 perform almost same in terms of packet delivery ratio, while perform better as compared to the state-of-the-art protocols because of consideration of route load balancing factor. It is clearly illustrated that stability and load balancing must be prioritize for heavy traffic in order to improve packet delivery ratio.

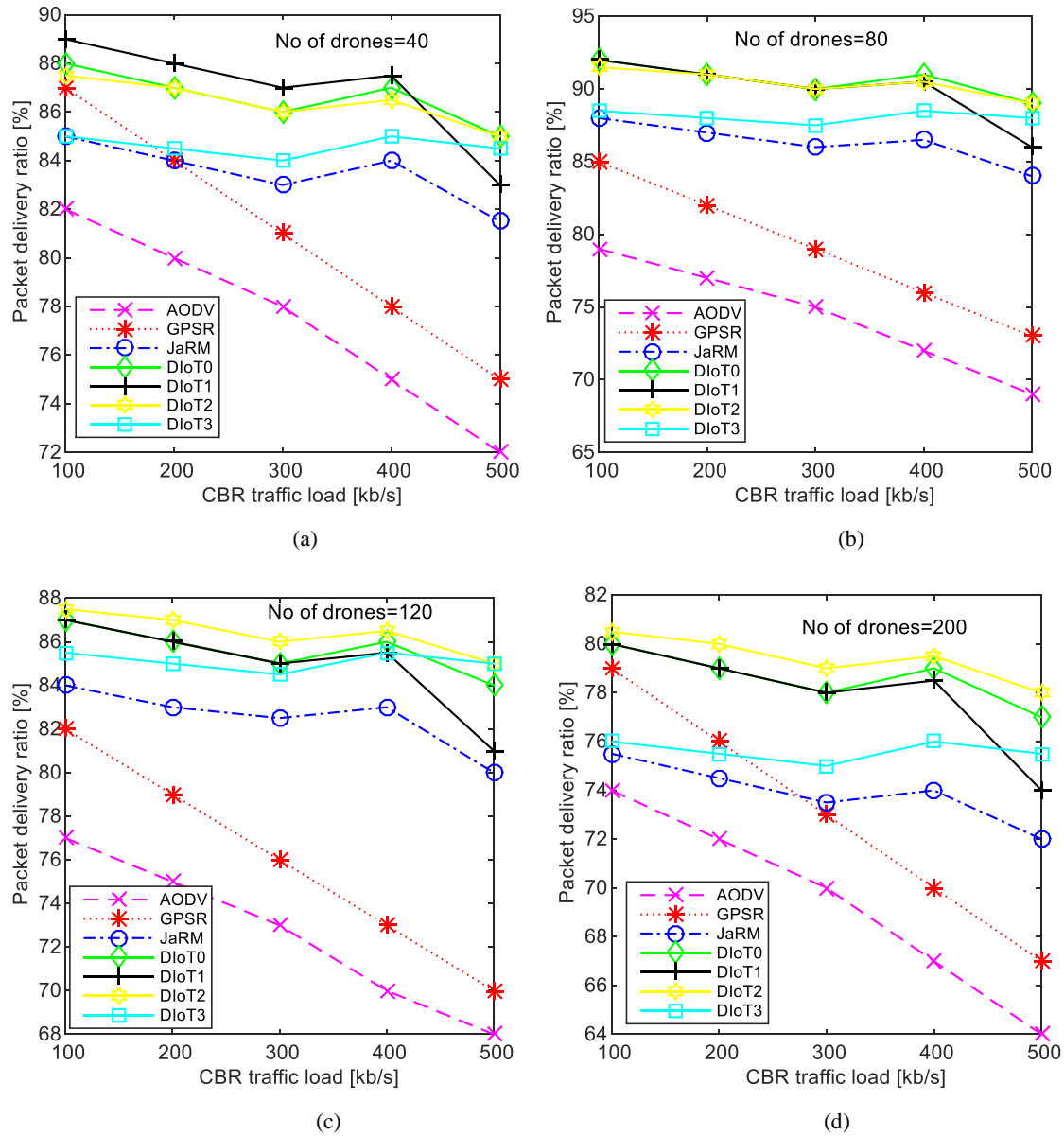


Fig.15.Variation in PDR and Traffic load when Number of drones are (a) 40, (b) 80, (c) 120 and (d) 200

Fig.16 shows the behavior of D-IoT in all scenarios in terms of number of handoffs (stability) while varying the departure gap of drones and number of drones. In fig. 16(a), 16(b), 16(c) and 16(d) performance metrics: number of handoffs and departure gap between drones are compared, when



Cite As:

Kumar, K., Kumar, S., Kaiwartya, O., Kashyap, P.K., Lloret, J. and Song, H., 2020. Drone assisted flying ad-hoc networks: mobility and service oriented modeling using neuro-fuzzy. *Ad Hoc Networks*, 106, p.102242.

number of drones are considered as 40, 80, 120 and 200 respectively. As shown in all scenarios of figure 16, average handoffs per hour increase (stability decreases) with the increment in number of drones in case of all protocols. It is also illustrated from fig.16 that handoffs/hour is inversely proportion to departure gap because handoffs/hour reduce when departure gap increases in case of all protocols. In case of D-IoT1, number of handoffs are slightly lesser as compared to D-IoT0, but in case of D-IoT2 and D-IoT3, are slightly higher than D-IoT0. But D-IoT in all scenarios performs much better than AODV and GPSR in terms of number of handoffs because no path stability metric is considered in case of GPSR and AODV. But JaRM performs better than AODV and GPSR in terms of average handoffs per hour, because path stability metric is utilized in case of JaRM. Still D-IoT in all scenarios performs better than JaRM.

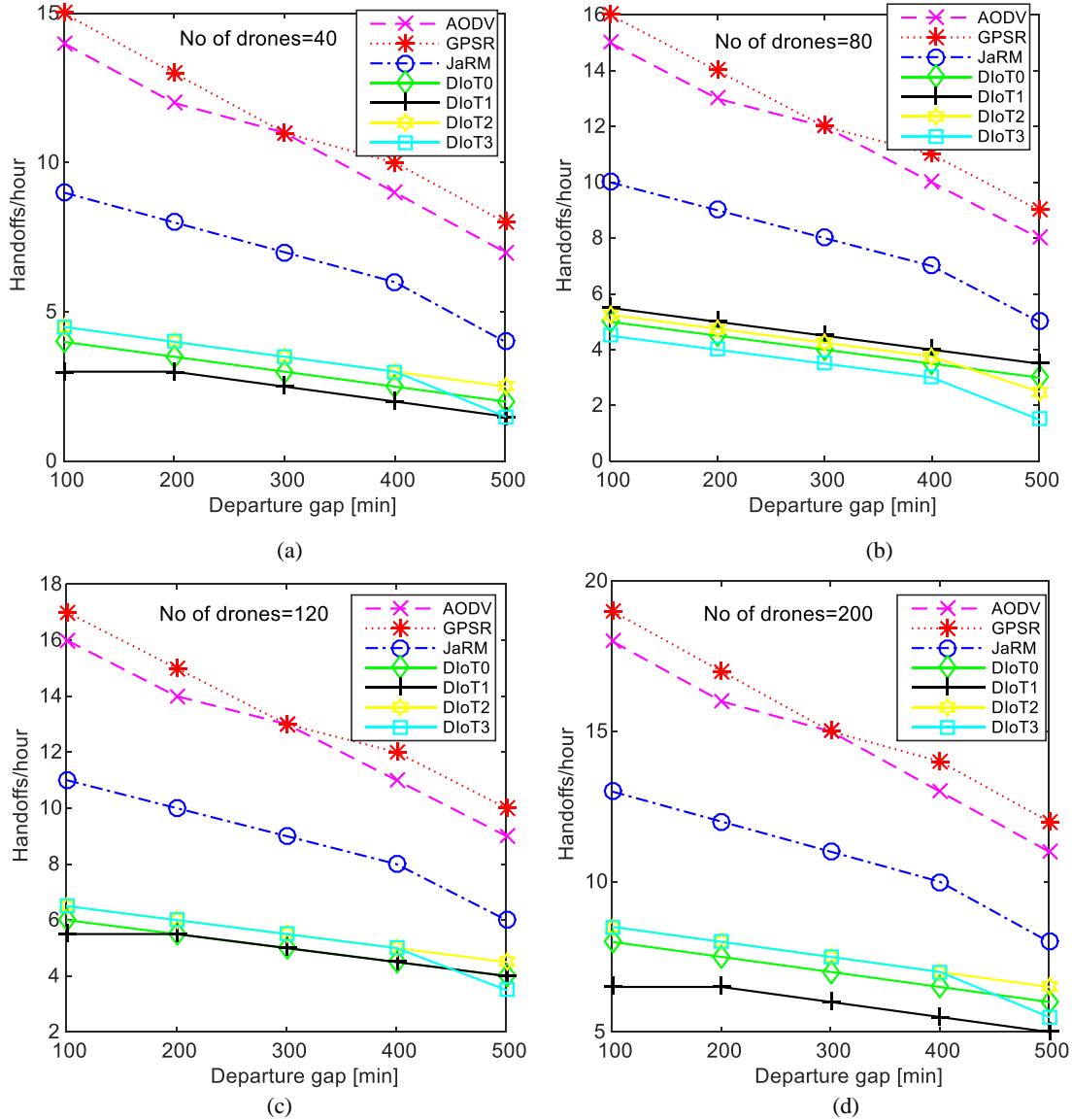


Fig.16.Variation in Handoffs and Departure gap when Number of drones are (a) 40, (b) 80, (c) 120 and (d) 200

The results in fig.16 illustrates the variation in route delay with the increment in number of drones and CBR traffic load for all the scenarios of D-IoT. In fig. 17(a), 17(b), 17(c) and 17(d) performance metrics: route delay and traffic load are compared, when number of drones are considered as 40, 80, 120 and 200 respectively. As shown in all scenarios of figure 16, route delay is proportional to number of drones because route delay increases when number of drones increase in case of all

Cite As:

Kumar, K., Kumar, S., Kaiwartya, O., Kashyap, P.K., Lloret, J. and Song, H., 2020. Drone assisted flying ad-hoc networks: mobility and service oriented modeling using neuro-fuzzy. *Ad Hoc Networks*, 106, p.102242.

protocols. It is also illustrated from fig.17 that for particular number of drones, route delay increases with the increment in traffic load. From all scenarios of fig.17, it is clearly enunciated that D-IoT3 outperforms D-IoT0, D-IoT1, D-IoT2, JaRM and GPSR, because in D-IoT3 highest priority is given to route delay. But D-IoT3 has slightly higher route delay as compared to AODV because packets are forwarded through shortest path in case of AODV, but is unstable. Still, D-IoT0, D-IoT1, D-IoT2 has better performance than GPSR and JaRM in terms of route delay because of consideration of local dynamic queue delay for node which avoids the congestion.

The results considering different weight factors show the enhancement in route stability, route delay and packet delivery ratio considering various scenarios inside the network.

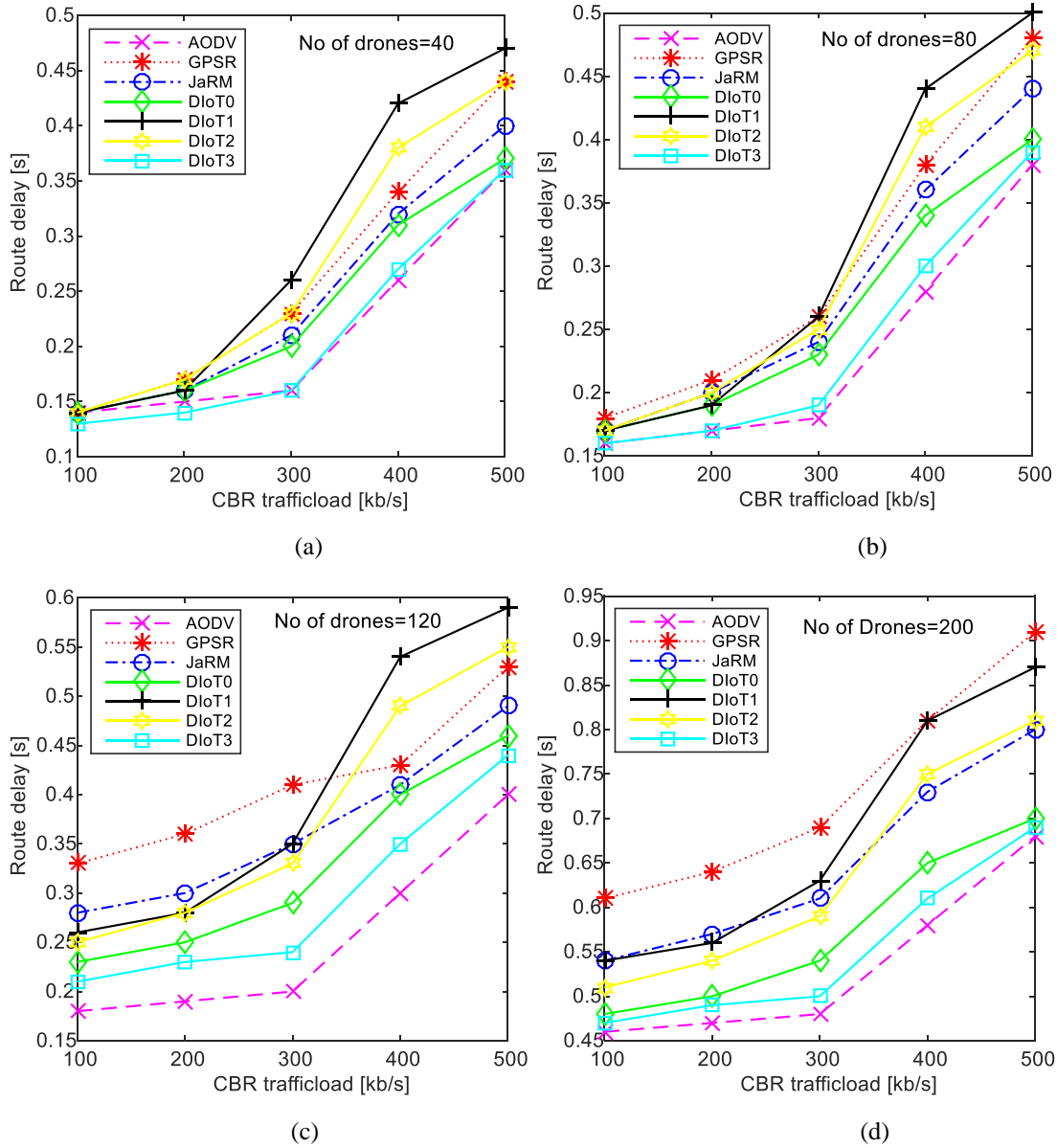


Fig.17. Variation in Route delay and Traffic load when Number of drones are (a) 40, (b) 80, (c) 120 and (d) 200

#### 4.1.2 Summary of Observations

The following lessons are learned from the design, implementation and analysis of the results. To provide efficient communication between drones and ground stations while having higher Quality of service parameters in highly mobile drone assisted Flying ad-hoc networks is a great challenge. Hence, the proposed drone assisted distributed routing framework focusing on quality of service provision in drone assisted IoT environments (D-IoT) enhances the network performance. Neuro-fuzzy interference system provides the reliable, balanced and efficient route selection by combining three important QoS provisioning parameters: route availability factor, residual route load capacity and route delay.

For comparative performance analysis, few traditional ad hoc networking framework and a recent drone framework were considered including AODV, GPSR, and JaRM. Further, metrics considered in the experimental results analysis includes packet delivery ratio, number of handoffs among Drones assisted Flying ad hoc networks, overhead and route delay. It is clarified that mathematical modeling derivation in Section 3 are the basis of considering these metrics in the analysis of results. Similar metrics were also considered in recent development in literature on drone assisted FANET environments. The analysis of experimental results is done firstly, based on equal weight assignment for QoS metrics and secondly, varying weight assignment for QoS metrics. As departure gap increases packet delivery ratio increases till departure gap threshold, after that packet delivery ratio starts decreasing. D-IoT outperforms the state-of-the-art protocols in terms of packet delivery ratio, because D-IoT could select next hop with the shortest queue of packets among all the possible nodes. Thus, this results the avoidance of local blocking.

The impact of traffic load is negative on packet delivery ratio. Packet delivery ratio with varying traffic load and number of drones is higher in case of proposed D-IoT than state-of-the-art protocols because of consideration of route load balancing factor in the proposed D-IoT. As departure gap increases overhead decreases, but when number of drones increase then overhead also increases. Best advertisement-based forwarding scheme used in D-IoT reduces overhead in case of D-IoT as compared to AODV and JaRM. But GPSR results less overhead as compared to D-IoT, because of utilization of smaller periodic hello packet for neighbor discovery in GPSR as compared to IGAD packet of D-IoT. Average number of handoffs increases as number of drones increases. Further with the increment in number of drones, there is slow and less increment in the number of handoffs in case of D-IoT as compared to state-of-the-art protocol. This is because, the more the drones, the larger air communication traffic, and then, D-IoT is more likely to find the next hop more stable with less node delay.

Route delay is proportional to both number of drones and traffic load in all compared protocols. Route delay in case of D-IoT is lower than GPSR and JaRM because route delay is considered as one of the route selection metrics in D-IoT, but not in GPSR and JaRM. D-IoT also considers local dynamic queue delay for node which avoids the congestion. Whereas, D-IoT has slightly higher route delay as compared to AODV because packets are forwarded through shortest path in case of AODV, but is unstable.

## 5. Conclusion

In this paper, a drone assisted distributed routing framework focusing on QoS provision (D-IoT) is presented for the enhancement of the network performance in IoT environment. A network model for drone assisted IoT environment is presented focusing the topological aspects of aerial drones and its mobility in flying ad hoc networks. To optimize Drone network centric QoS provisioning parameters are derived focusing on relative velocity of drones, expected link availability period, residual route load capacity and route delay. Neuro-fuzzy interference system has been employed to jointly combine three important QoS provisioning parameters to assist in reliable and efficient route selection. A drone assisted distributed routing framework is developed based on the drone mobility model and QoS parameters. The proposed communication framework is tested to comparatively

Cite As:

Kumar, K., Kumar, S., Kaiwartya, O., Kashyap, P.K., Lloret, J. and Song, H., 2020. Drone assisted flying ad-hoc networks: mobility and service oriented modeling using neuro-fuzzy. *Ad Hoc Networks*, 106, p.102242.

evaluate the performance with the state-of-the-art protocols considering metrics related to flying ad-hoc networks environments. The simulation results show that D-IoT outperforms the state-of-the-arts protocols. It is highlighted that the proposal can be utilized for any applications of drone assisted adhoc networking such as enabling agriculture and traffic related services using drones. Further, the framework can be also utilized in drone assisted border monitoring. However, reliability centric development needs to be added before using it for security-oriented drone monitoring applications. In the future research, the authors will focus on consideration of energy utilization as performance metric including the design modification. The authors will also explore the work in diverse scenarios, and applications.

## References

- [1] O. Kaiwartya, Abdullah, A.H., Cao, Y., Altameem, A., Prasad, M., Lin, C.T. and Liu, X., "Internet of Vehicles: Motivation, Layered Architecture, Network Model, Challenges, and Future Aspects," in *IEEE Access*, vol. 4, pp. 5356-5373, 2016.
- [2] M. Asif-Ur-Rahman, Afsana, F., Mahmud, M., Kaiser, M.S., Ahmed, M.R., Kaiwartya, O. and James-Taylor, A., "Towards a Heterogeneous Mist, Fog, and Cloud based Framework for the Internet of Healthcare Things," in *IEEE Internet of Things Journal*.
- [3] C. C. Baseca, J. R. Díaz and J. Lloret, "Communication Ad Hoc Protocol for Intelligent Video Sensing Using AR Drones," *2013 IEEE 9th International Conference on Mobile Ad-hoc and Sensor Networks*, Dalian, 2013, pp. 449-453.
- [4] B. Yu, J. Wright, S. Nepal, L. Zhu, J. Liu and R. Ranjan, "IoTChain: Establishing Trust in the Internet of Things Ecosystem Using Blockchain," in *IEEE Cloud Computing*, vol. 5, no. 4, pp. 12-23, Jul./Aug. 2018.
- [5] M. Fazio, R. Ranjan, M. Girolami, J. Taheri, S. Dustdar and M. Villari, "A Note on the Convergence of IoT, Edge, and Cloud Computing in Smart Cities," in *IEEE Cloud Computing*, vol. 5, no. 5, pp. 22-24, Sep./Oct. 2018.
- [6] T. Rausch, S. Dustdar and R. Ranjan, "Osmotic Message-Oriented Middleware for the Internet of Things," in *IEEE Cloud Computing*, vol. 5, no. 2, pp. 17-25, Mar./Apr. 2018..
- [7] Schnell, M. and Scalise, S; "NEWSKY-Concept for networking the SKY for civil aeronautical communications" *IEEE Aerosp. Electron. Syst.Mag.*, vol.22, no.5, pp.25-29, 2007.
- [8] F De Rango, G Potrino, M Tropea, AF Santamaria, P Fazio, "Scalable and lighthway bio-inspired coordination protocol for FANET in precision agriculture applications," in *Computers & Electrical Engineering*, Vol. 74, 2019, pp.305-318.
- [9] Tropea, M., Santamaria, A. F., De Rango, F., & Potrino, G. (2019, January). Reactive flooding versus link state routing for FANET in precision agriculture. In *2019 16th IEEE Annual Consumer Communications & Networking Conference (CCNC)* (pp. 1-6). IEEE.
- [10] Kaiwartya, O., Abdullah, A.H., Cao, Y., Raw, R.S., Kumar, S., Lobiyal, D.K., Isnin, I.F., Liu, X. and Shah, R.R., T-MQM: Testbed-based multi-metric quality measurement of sensor deployment for precision agriculture—A case study. *IEEE Sensors Journal*, 16(23), pp.8649-8664, 2016.
- [11] M. De Sanctis, E. Cianca, G. Araniti, I. Bisio and R. Prasad, "Satellite Communications Supporting Internet of Remote Things," in *IEEE Internet of Things Journal*, vol. 3, no. 1, pp. 113-123, Feb. 2016.
- [12] A Bujari, CE Palazzi, D Ronzan, "A comparison of stateless position-based packet routing algorithms for FANETs," in *IEEE Transactions on Mobile Computing* 17 (11), 2018, pp. 2468-2482.
- [13] Garcia, F.; Pirovano, A.; Royer, M. and Vey, Q. "Aeronautical air-ground data communication: Current and future trends", in *Clean Mobility and Intelligent Transport Systems*, London, U.K., IET Digit. Libr., pp.40-416, 2015.
- [14] Vey, Q.; Pirovano, A.; Radzik, J. and Garcia, F; "Aeronautical ad hoc network for civil aviation," in *Communication Technologies for Vehicles*. Springer, pp. 81–93, 2014.
- [15] E. Sakhaee and A. Jamalipour, "The Global In-Flight Internet," in *IEEE Journal on Selected*

Cite As:

Kumar, K., Kumar, S., Kaiwartya, O., Kashyap, P.K., Lloret, J. and Song, H., 2020. Drone assisted flying ad-hoc networks: mobility and service oriented modeling using neuro-fuzzy. *Ad Hoc Networks*, 106, p.102242.

Areas in Communications, vol. 24, no. 9, pp. 1748-1757, 2006.

- [16] Perkins, C.; Belding-Royer, E. and Das, S; "Ad hoc on Demand Distance Vector (AODV) Routing," (RFC3561), Available online: <http://www.ietf.org/rfc/rfc3561.txt> (accessed on 30 January 2013).
- [17] Karp, B. and Kung, H.T; "GPSR: Greedy perimeter stateless routing for wireless networks," in Proc. 6th ACM Int.Conf. Mobile Comput. Netw., Boston, MA, USA, pp. 243–254, 2000.
- [18] E. Sakhaee and A. Jamalipour, "Stable Clustering and Communications in Pseudolinear Highly Mobile Ad Hoc Networks," in *IEEE Transactions on Vehicular Technology*, vol. 57, no. 6, pp. 3769-3777, Nov. 2008.
- [19] Medina, D.; Hoffmann, F.; Rossetto, F. and Rokitansky, C. H; "A geographic routing strategy for North Atlantic in-flight Internet access via airborne mesh networking," *ACM Trans. Netw.*, vol. 20, no. 4, pp. 1231–1244, 2012
- [20] Y. Li, R. Shirani, M. Hilaire, and T. Kunz, "Improving routing in networks of Unmanned Aerial Vehicles: Reactive-Greedy-Reactive," *Wirel. Commun. Mob. Comput*, vol. 12, no. 18, pp. 1608-1619, 2012.
- [21] G. Tuna, B. Nefzi, G. Conte, "Unmanned aerial vehicle-aided communications system for disaster recovery," *Journal of Network and Computer Applications*, vol. 41, pp.27-36, 2014.
- [22] Y. Liu, Z. Luo, Z. Liu, J. Shi and G. Cheng, "Cooperative Routing Problem for Ground Vehicle and Unmanned Aerial Vehicle: The Application on Intelligence, Surveillance, and Reconnaissance Missions," in *IEEE Access*, vol. 7, pp. 63504-63518, 2019.
- [23] F. Aftab, A. Khan and Z. Zhang, "Hybrid Self-Organized Clustering Scheme for Drone Based Cognitive Internet of Things," in *IEEE Access*, vol. 7, pp. 56217-56227, 2019.
- [24] C. Cambra, S. Sendra, J. Lloret, L. Parra, "Ad hoc network for emergency rescue system based on unmanned aerial vehicles," *Network Protocols and Algorithms* 7 (4), pp.72-89. 2015.
- [25] I. Garcia-Magarino, G. Gray, R. Lacuesta and J. Lloret, "Smart Green Communication Protocols Based on Several-Fold Messages Extracted from Common Sequential Patterns in UAVs," in *IEEE Network*, 2020, doi: 10.1109/MNET.001.1900417.
- [26] M. Y. Arafat and S. Moh, "Localization and Clustering Based on Swarm Intelligence in UAV Networks for Emergency Communications," in *IEEE Internet of Things Journal*. doi: 10.1109/IIOT.2019.2925567.
- [27] Lei, L.; Wang, D.; Zhou, L.; Chen, X.; and Cai, S; "Link availability estimation based reliable routing for aeronautical ad hoc networks," *Ad Hoc Netw.*, vol. 20, pp. 53–63, 2014.
- [28] F. Hoffmann, D. Medina and A. Wolisz, "Joint Routing and Scheduling in Mobile Aeronautical Ad Hoc Networks," in *IEEE Transactions on Vehicular Technology*, vol. 62, no. 6, pp. 2700-2712, July 2013.
- [29] K. Peng *et al.*, "A Hybrid Genetic Algorithm on Routing and Scheduling for Vehicle-Assisted Multi-Drone Parcel Delivery," in *IEEE Access*, vol. 7, pp. 49191-49200, 2019.
- [30] K. Dorling, J. Heinrichs, G. G. Messier and S. Magierowski, "Vehicle Routing Problems for Drone Delivery," in *IEEE Transactions on Systems, Man, and Cybernetics: Systems*, vol. 47, no. 1, pp. 70-85, Jan. 2017.
- [31] M. Hu *et al.*, "Joint Routing and Scheduling for Vehicle-Assisted Multidrone Surveillance," in *IEEE Internet of Things Journal*, vol. 6, no. 2, pp. 1781-1790, April 2019.
- [32] Q. Fan and N. Ansari, "Towards Traffic Load Balancing in Drone-Assisted Communications for IoT," in *IEEE Internet of Things Journal*, vol. 6, no. 2, pp. 3633-3640, April 2019.
- [33] M. Asadpour, K. A. Hummel, D. Giustiniano and S. Draskovic, "Route or Carry: Motion-Driven Packet Forwarding in Micro Aerial Vehicle Networks," in *IEEE Transactions on Mobile Computing*, vol. 16, no. 3, pp. 843-856, 1 March 2017.
- [34] Avellar, G.S.C.; Pereira, G.A.S.; Pimenta, L.C.A.; Iscold, P. Multi-UAV Routing for Area Coverage and Remote Sensing with Minimum Time. *Sensors* 2015, 15, 27783-27803.
- [35] C. Pu, "Jamming-Resilient Multipath Routing Protocol for Flying Ad Hoc Networks," in *IEEE Access*, vol. 6, pp. 68472-68486, 2018.
- [36] P. Yang, X. Cao, X. Xi, W. Du, Z. Xiao and D. Wu, "Three-Dimensional Continuous Movement Control of Drone Cells for Energy-Efficient Communication Coverage," in *IEEE Transactions on Vehicular Technology*, vol. 68, no. 7, pp. 6535-6546, July 2019.

Cite As:

Kumar, K., Kumar, S., Kaiwartya, O., Kashyap, P.K., Lloret, J. and Song, H., 2020. Drone assisted flying ad-hoc networks: mobility and service oriented modeling using neuro-fuzzy. *Ad Hoc Networks*, 106, p.102242.

- [37] Ahmed, M.N., Abdullah, A.H., Chizari, H. and Kaiwartya, O., 2017. F3TM: Flooding Factor based Trust Management Framework for secure data transmission in MANETs. *Journal of King Saud University-Computer and Information Sciences*, 29(3), pp.269-280.
- [38] Kaiwartya, O. and Kumar, S., 2014. Enhanced caching for geocast routing in vehicular Ad Hoc network. In *Intelligent computing, networking, and informatics* (pp. 213-220). Springer, New Delhi.
- [39] Qureshi, K.N., Abdullah, A.H., Kaiwartya, O., Ullah, F., Iqbal, S. and Altameem, A., 2016. Weighted link quality and forward progress coupled with modified RTS/CTS for beaconless packet forwarding protocol (B-PFP) in VANETs. *Telecommunication Systems*, pp.1-16.
- [40] Cao, Y., Kaiwartya, O., Aslam, N., Han, C., Zhang, X., Zhuang, Y. and Dianati, M., 2018. A trajectory-driven opportunistic routing protocol for VCPS. *IEEE Transactions on Aerospace and Electronic Systems*, 54(6), pp.2628-2642.
- [41] F De Rango, M Tropea, P Fazio, "Bio-Inspired Routing over FANET in Emergency Situations to support Multimedia Traffic," in *Proc. of the ACM MobiHoc workshop on innovative aerial communication solutions for First REsponders network in emergency scenarios*, 2019, pp.12-17.
- [42] B. Liang and Z. J. Haas, "Predictive distance-based mobility management for multidimensional PCS networks," in *IEEE/ACM Transactions on Networking*, vol. 11, no. 5, pp. 718-732, 2003.
- [43] J. S. R. Jang, "ANFIS: adaptive-network-based fuzzy inference system," in *IEEE Transactions on Systems, Man, and Cybernetics*, vol. 23, no. 3, pp. 665-685, 1993.
- [44] Li, J., Yang, L., Qu, Y., Sexton, G., 2018. An extended Takagi–Sugeno–Kang inference system (TSK+) with fuzzy interpolation and its rule base generation. *Soft Computing*, 22, pp.3155–3170.
- [45] Nekrasov, M.; Allen, R.; Artamonova, I.; Belding, E. Optimizing 802.15.4 Outdoor IoT Sensor Networks for Aerial Data Collection. *Sensors* 2019, 19, 3479. 2.